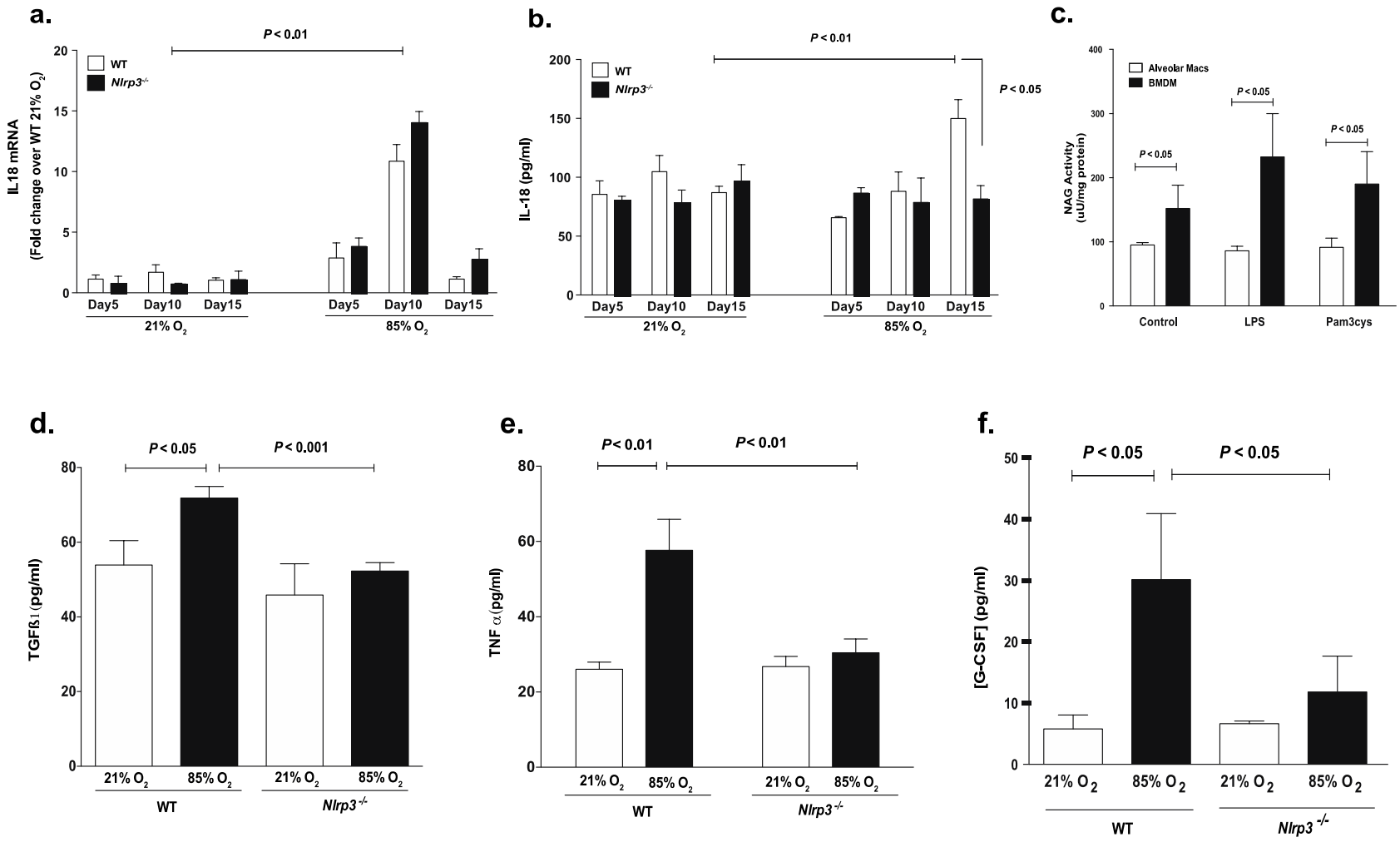

Supplementary Figure 1: *Nlrp3*$^{-/-}$ mice are protected from increases in IL18, TGFß1 and TNFα observed with exposure to hyperoxia in WT mice. All data are expressed as mean ± s.e.m., with *n* = 6-12 animals per group for each experiment. (**a**). Animals kept in 21% O_2 showed no increases in IL18 mRNA. Exposure to 85% O_2 resulted in changes in IL18 mRNA that mimicked those seen with IL1ß mRNA, significantly increasing at PN10 in both WT and *Nlrp3*$^{-/-}$ mice. (**b**). IL18 protein increased in the BAL of WT mice exposed to 85% O_2, but no increases were noted in mice kept in 21% O_2, or in *Nlrp3*$^{-/-}$ mice exposed to 85% O_2. (c). NAG activity was compared between resident alveolar macrophages and bone marrow-derived macrophages (BMDM) under quiescent conditions and after treatment with LPS or Pam3Cys. Increased NAG activity was only found in BMDM under all three conditions (**d, e & f**). Exposure to 85% O_2 increased the expression of active TGFß1 (**d**), TNFα (**e**) and G-CSF (**f**) in the BAL of WT mice obtained on PN15. However, *Nlrp3*$^{-/-}$ mice failed to show any increases in TGFß1, TNFα, or G-CSF with hyperoxia exposure.

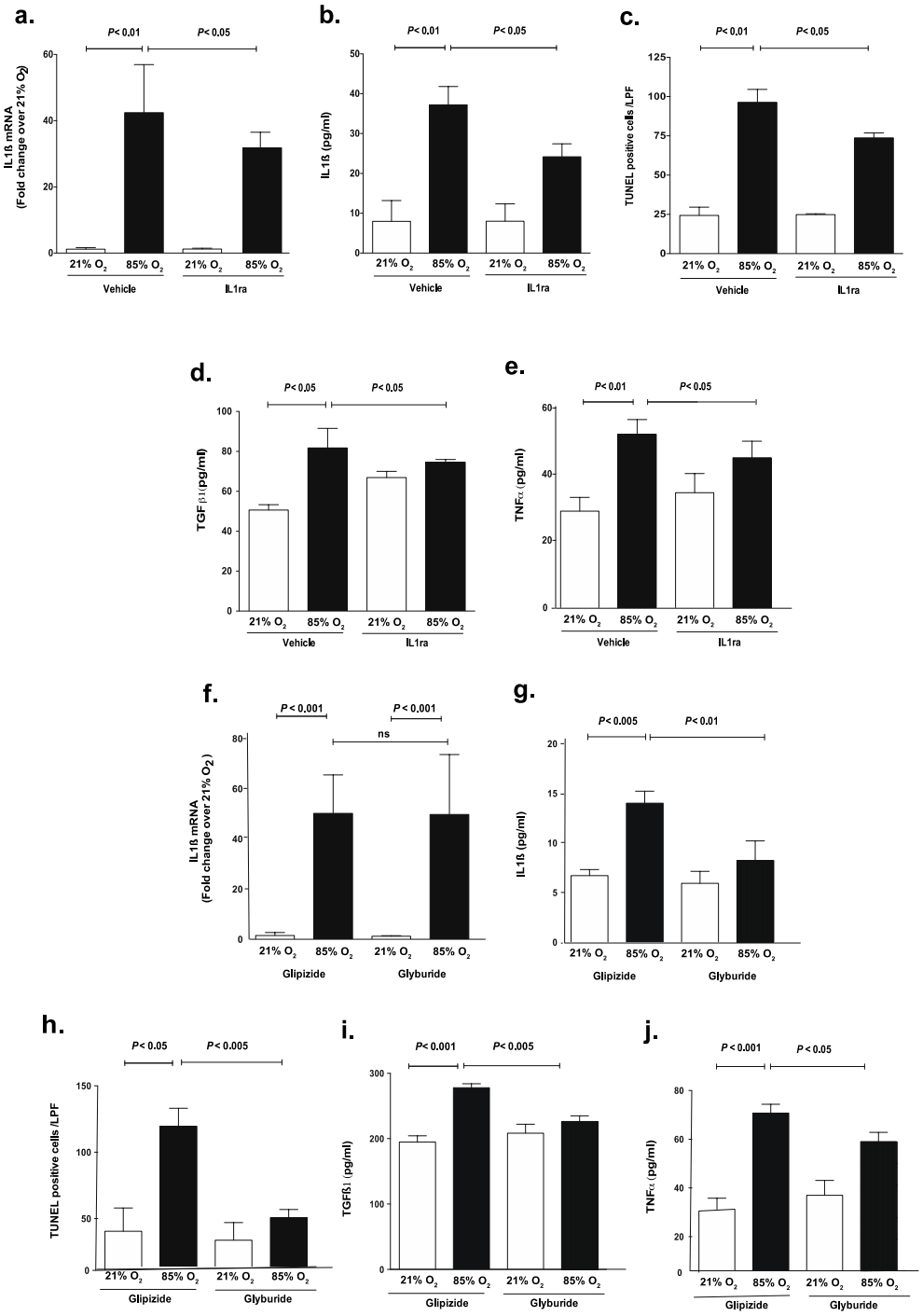

Supplementary Figure 2: Effects on IL1ß mRNA, IL1ß protein, TUNEL-positive cells, TGFß1 and TNFα in WT mice exposed to 21% or 85% O_2 treated with either recombinant IL1ra (**a-e**) or glyburide (**f-j**), using vehicle or glipizide as controls respectively. All data are expressed as mean ± s.e.m., with *n* = 6-12 animals per group for each experiment. (**a**). Exposure to 85% O_2 was associated with increase in IL1ß mRNA in both vehicle and IL1ra-treated mice. IL1ra-treated mice had lower IL1ß mRNA than vehicle-treated mice exposed to 85% O_2. (**b**). Exposure to 85% O_2 was associated with increase in IL1ß protein in both vehicle and IL1ra-treated mice. IL1ra-treated mice had lower IL1ß protein than vehicle-treated mice exposed to 85% O_2. (**c**). Vehicle-treated mice exposed to 85% O_2 had increased TUNEL-positive cells. Treatment of hyperoxia-exposed mice with IL1ra was associated with a 30% decrease in the number of TUNEL-positive cells. (**d**). Vehicle-treated mice exposed to 85% O_2 had increased TGFß1 whereas IL1ra-treated mice had no increase in TGFß1 with hyperoxia exposure. (**e**). Vehicle-treated mice exposed to 85% O_2 had increased TNFα whereas IL1ra-treated mice had no increase in TNFα with hyperoxia exposure. (**f**). Exposure to 85% O_2 was associated with equally increased IL1ß mRNA in both glipizide- and glyburide-treated mice. (**g**). Compared to the two-fold increase in IL1ß protein content in glipizide-treated mice in 85% O_2, glyburide-treated mice had no increase in IL1ß. (**h**). Compared to the four-fold increase in TUNEL-positive cells in hyperoxia-exposed mice treated with glipizide, glyburide-treated mice had no increase in TUNEL positive cells. (**i-j**). Glipizide-treated mice exposed to 85% O_2 had increased TGFß1 (**i**) and TNFα (**j**). Glyburide treated hyperoxia-exposed mice did not show any increase in active TGFß1, and had a blunted increase in TNFα.

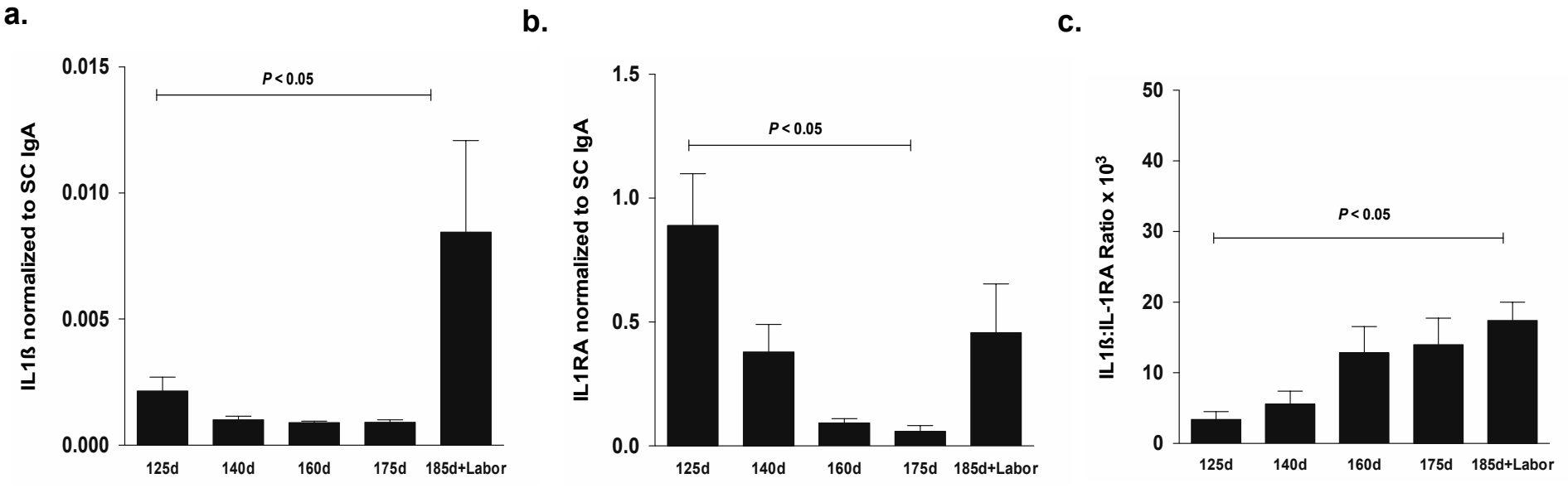

Supplementary Figure 3: Ontogeny of lung fluid IL1ß, IL1ra and IL1ß:IL1ra ratio during non-human primate gestation. Fetal baboons were harvested at specific times during gestation (125 days to 175 days) and at term with the onset of labor (185 days). All data are expressed as mean ± s.e.m., with *n* = 6-8 animals per group for each experiment. (**a**). IL1ß content normalized to SCIgA was low during gestation and increased significantly at term after the onset of labor. (**b**). IL1ra normalized to SCIgA decreased during gestation, and increased at term after the onset of labor. (**c**). IL1ß:ILra ratio gradually increased over time during gestation and was maximally increased at term gestation with labor.

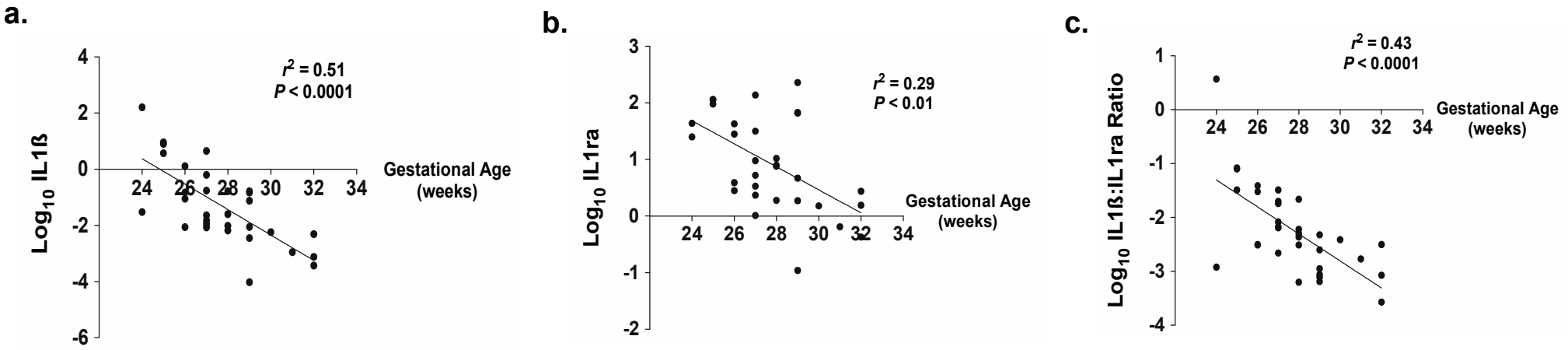

Supplementary Figure 4: Correlations of IL1ß, ILra and IL1ß:IL1ra ratio to gestational age. (**a-c**). Log transformed values of each biomarker from days 1-3 were plotted against gestational age and Pearson correlations determined. Each biomarker was significantly negatively correlated with gestational age.

Full Blot, Fig. 1d:

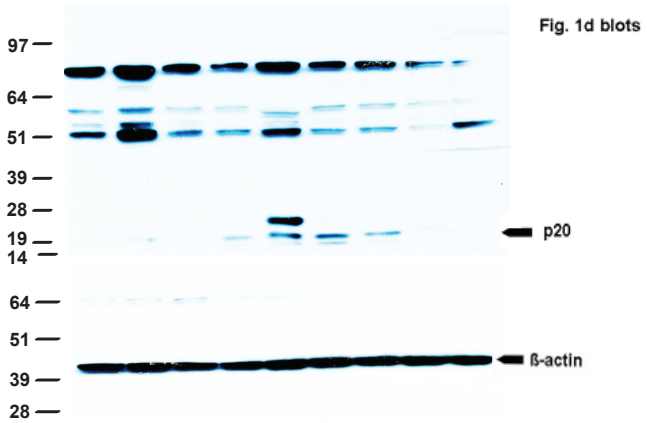

Full Blot, Fig. 2b:

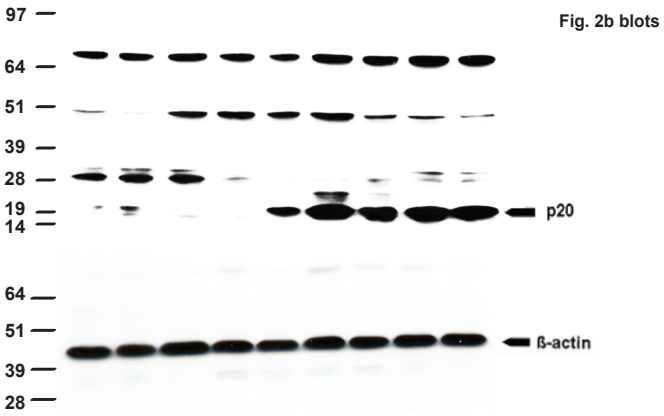

Full Blot, Fig. 2h:

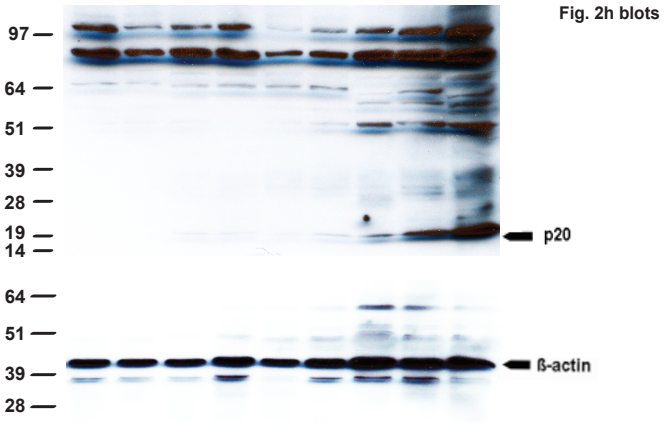

Full Blot, Fig. 3c:

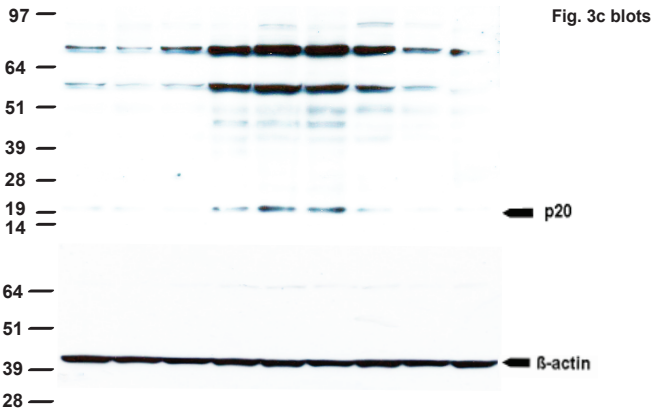

Supplementary Figure 5: Full Blots of Figures 1d, 2b, 2h and 3c together with the corresponding ß-actin loading control blots.